

Effects of water-depth mismatch on matched-field localization in shallow water

DTIC FILE COPY

DTIC
SELECTED
AUG 19 1988
E

Donald R. Del Balzo
Naval Ocean Research and Development Activity, NSTL, Mississippi 39529-5004

Christopher Feuillade and Mary M. Rowe^{a)}
SYNTEK/ODSI Defense Systems, Inc., 6110 Executive Boulevard, Rockville, Maryland 20852

(Received 30 October 1987; accepted for publication 25 January 1988)

This article discusses the impact of incorrect estimates of the water column depth on matched-field source localization in a shallow-water environment. Computer calculations were performed for the case of a nominal 100-m depth water column subject to water-depth variations of up to ± 3.5 m, which would be caused by long-period ocean swell or by tidal changes. The environment was assumed to be range independent (by proper choice of the geometry); thus the question of rough surface scattering was not an issue. The calculations incorporated source depths of 25, 50, and 75 m, a propagation distance of 4 km, an acoustic frequency of 150 Hz, and a linear vertical receiving array. The array consisted of 21 hydrophones with an interelement spacing of 2.5 m, and it spanned the center one-half of the water column (25- to 75-m depth). The matched-field algorithm utilized in this study is the high-resolution maximum-likelihood estimator. A primary result of the work is that, as the output of the matched-field processor degrades due to water-depth mismatch, the apparent source location varies in a systematic way; i.e., the source appears closer and deeper for increasing water depth and, conversely, the source appears farther and shallower for decreasing water depths. Another significant observation is that, as acoustic modes are stripped from the waveguide due to reduced channel depth, instabilities in the solution of the processor cause random variations in localization estimates.

PACS numbers: 43.30.Wi, 43.60.Gk

DTIC
COPY
INSPECTED
1

tion For	
GRA&I	<input checked="" type="checkbox"/>
TAB	<input type="checkbox"/>
ounced	<input type="checkbox"/>
ification	
tribution/	
liability Codes	
Dist	Avail and/or Special
A-1	21

AD-A198 001

INTRODUCTION

The use of matched-field techniques in underwater acoustic processing has been a subject of keen interest and debate over the last 2-3 years. Essentially, the technique involves the correlation of the acoustic pressure field detected at each receiver in a hydrophone array due to a submerged source, with the field calculated at the receiver based upon an estimated source position and an assumed model of the environment. A high degree of correlation between the experimental and model fields should indicate an increased probability of finding the source at the estimated position. For the vertical array geometry considered in this study, estimates of source range and depth are calculated and then displayed on a range-depth ambiguity surface.

A number of different mathematical estimator functions may be employed to make the comparisons between the experimental and model fields. An overview of a number of these functions has recently been given by Fizell.¹ Perhaps the most straightforward of these is a conventional cross correlation of the two sets of complex pressure values. A good discussion of this method has been given by Heitmeyer *et al.*²; and another similar technique has been described by Bucker.³

Much more attention has been given to the maximum-likelihood estimator, first introduced for use in a seismic

array by Capon *et al.*⁴ This method was adapted for depth estimation in a waveguide by Hinich⁵; and successful experimental trials employing it for localization in depth and range have been reported in shallow-water⁶ and deep-water, arctic⁷ environments. The maximum-likelihood estimator shows great promise as a high-resolution localization tool. However, there are some important questions to be answered concerning its robustness, reliability, and accuracy when the environmental data used to calculate the model acoustic pressure field are incomplete or inaccurate, so that a data "mismatch" occurs between the experimental and model pressure fields.

In this article, we investigate the consequences, for the maximum-likelihood function, of one important type of error that arises due to a mismatch in the water depth, as illustrated schematically in Fig. 1. The problem is considered for an acoustic frequency of 150 Hz (10-m wavelength) and realistic water-depth mismatches of up to ± 3.5 m, which are typical of sea swell and tidal variations. Since the degree of mismatch is a large fraction of an acoustic wavelength, it is expected that the acoustic pressure field at the individual hydrophones will be greatly affected. Therefore, the cross correlation between the nominal and perturbed fields will be degraded, and errors in localization may be expected. The localization sensitivity to water-depth mismatch is systematically examined in this article for a range-independent environment, i.e., no rough surface scattering.

^{a)} Present address: Naval Ocean Research and Development Activity.

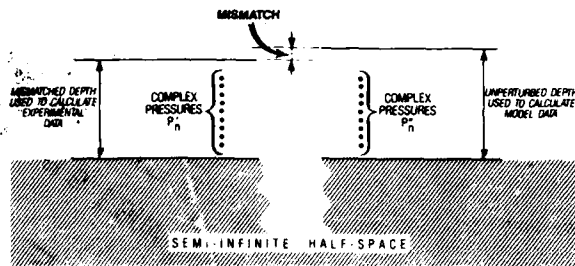


FIG. 1. Water-depth mismatch problem.

I. THEORY

As mentioned above, the matched-field technique considered here is the maximum-likelihood estimator. For a full description of this method, the reader is referred to a standard text (e.g., Ref. 8). Here, we will provide only a brief summary of the basic theory as applied to the specific problem of a vertical receiving array and a submerged source.

Let the complex acoustic pressure field recorded at the n th element of a vertical hydrophone array due to a source located at depth and range (z_0, r_0) be given by P_n'' . We may write down a matrix row vector \tilde{X} (the tilde denotes the transpose) of length N (the total number of hydrophones) whose individual elements are the pressure fields recorded at those hydrophones, i.e.,

$$\tilde{X} = (P_1'', P_2'', \dots, P_N''). \quad (1)$$

From this, we may form the cross-spectral (or covariance) matrix

$$R = \tilde{X}X^\dagger, \quad (2)$$

where \dagger denotes the adjoint vector. In an experimental test, a mean cross-spectral matrix would be found by averaging over the total number M of recorded time samples:

$$\bar{R} = \frac{1}{M} \sum_{k=1}^M R_k, \quad (3)$$

where R_k is the cross-spectral matrix for the k th time sample. In the simulation study discussed here, noise on the hydrophones is simulated by adding a constant to each of the main diagonal elements of R . This constant is scaled to give the desired signal-to-noise ratio. This simple approach for adding noise to the problem corresponds to a deterministic, uncorrelated noise field with an infinite time-bandwidth product. This type of noise assumption produces a noise floor on the ambiguity surfaces without introducing any structure. All of the variations on the range-depth ambiguity surfaces are due to signal characteristics for the environment under study. This simplifies the analysis of source localization as affected by environmental uncertainty.

Now consider another row vector \bar{E} , whose members are the complex pressure fields P_n'' calculated at each hydrophone due to an estimated source position (\hat{z}_0, \hat{r}_0) , and normalized to unity. Therefore,

$$\bar{E} = (\bar{P}_1'', \bar{P}_2'', \dots, \bar{P}_N''), \quad (4)$$

where

$$\bar{P}_n'' = P_n'' / \left(\sum_{i=1}^N |P_i''|^2 \right)^{1/2}. \quad (5)$$

Now the maximum-likelihood function may be written

$$L(z_0, \hat{z}_0; r_0, \hat{r}_0) = 1/[E^\dagger(\bar{R})^{-1}E]. \quad (6)$$

We can see from the matrix expression in the denominator of Eq. (6) that determination of the value of the maximum-likelihood function involves calculating products of functions of the model pressure field \bar{P}_n'' (in E) and functions of the measured pressure field P_n'' (in R). If the model field and measured field correspond closely with each other for every individual hydrophone, then the denominator in Eq. (6) will be small, and, hence, L will take a large value. However, if a mismatch in the water depth comparable to the hydrophone spacing occurs, then a significant phase error will be introduced into the calculated model value of the pressure field at each hydrophone. These may then differ seriously from the measured field values for the corresponding hydrophones, leading to a detrimental effect on the value of L calculated in Eq. (6).

The likelihood function can be displayed in the form of a range-depth ambiguity surface. High values of correlation indicate likely positions of sources. The source localization procedure is to search all possible range-depth coordinates for a maximum value.

II. ENVIRONMENTAL MODEL

The geoaoustic environmental model used in this work is the two-layered liquid half-space model pioneered by Pekeris.⁹ The model consists of a shallow isospeed water layer of uniform density overlying a faster, isospeed, semi-infinite fluid bottom of uniform (and usually higher) density. For a full description of the general Pekeris model, the reader is referred to a standard text (e.g., Ref. 10). In this work, the water depth is 100 m, the sound speed in the water and sediment is 1500 and 1621.6 m/s, respectively, and the sediment/water density ratio is 1.772. Even though the simplicity of the Pekeris model limits its general applicability, it does possess features that are very similar to at least one shallow-water environment in which matched-field experiments have been performed.⁶ In this case, the water sound-speed profile was almost isospeed, and a thick sandy sediment layer was present, which carried no shear waves and, therefore, behaved like a fluid. The Pekeris model is also a widely used and well-understood standard model. It should describe most of the acoustic phenomena that result from changes in the water depth for shallow-water environments. Since the acoustic wavefunctions within the waveguide are calculated analytically, without need for recourse to numerical techniques, the calculation of the maximum-likelihood function in Eq. (6) is greatly facilitated, making the Pekeris model an excellent choice for our present purposes.

III. SEA-SURFACE MODEL

It is clear that the variations in surface wave height under typical sea conditions will be generally random and difficult to model analytically. There are no standard propagation codes that allow for the introduction of randomly

varying wave height readily available at the present time. In order, therefore, to consider the problem of the effect of variable water depth (due to surface waves) on the maximum-likelihood estimator using the Pekeris model, we have made two simplifying assumptions. The first of these is to study the effects of water-depth mismatch due to long-period ocean swell. The results apply equally well to water-depth changes induced by tidal forces. The relationship between wind waves and swell has been the subject of extensive investigation, and a comprehensive review of it has been given by Wiegel.¹¹ Since the ocean is a dispersive medium as far as surface waves are concerned, waves of different periods generated by a storm travel away from it at different speeds. The waves with the longest period travel most quickly. At a distance of a few storm diameters from their origin, the waves will propagate independently of each other, and are characterized by a sinusoidal waveform on the ocean surface. In this work, we have considered the effects of an ocean swell with peak-to-trough amplitude of 7 m. Since this is about the greatest swell amplitude recorded,¹² we may consider it a "worst case" estimate.

The second simplification is to utilize a "long-crested" model of the ocean surface, and to assume a geometry in which sound propagates from the source to the array of receivers along paths parallel to the crests, as shown in Fig. 2. Since we are considering a source-receiver range of 4 km, we are dealing with acoustic transit times of less than 3 s. Earle *et al.*¹² have reported that swells on the order of the amplitude considered in this article have periods of about 20–25 s. Hence, it seems reasonable to use a "frozen ocean" assumption and to neglect the small change in surface height that occurs as the signal propagates from the source to the hydrophone array along the ocean crests.

The primary results of this article involve localization errors induced by water-depth mismatch for the individual wave-height cases. Therefore, these results similarly apply to water-depth mismatch caused by the quasistatic situation of tidal forces. A secondary result concerns the average effect of water-depth mismatch during the passage of a long-period wave. This result stems from the calculation of the mean of a series of range-independent, static cases, each representing a different phase of the surface wave.

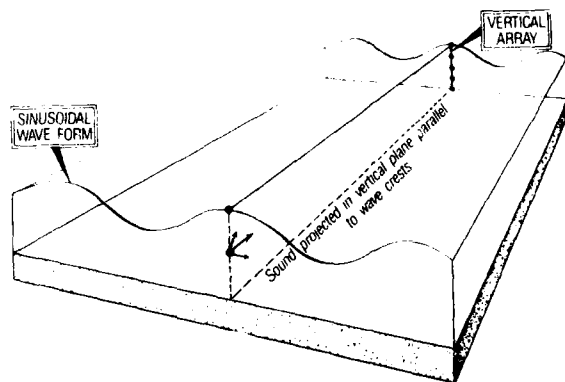


FIG. 2. Long-crested model of sinusoidally varying ocean surface.

IV. ANALYSIS PROCEDURE

In this article, we consider the localization of a 150-Hz source placed at depths of 25, 50, and 75 m in a waveguide of water depth 100 m, at a range of 4 km from a linear vertical array. The receiver array consists of 21 hydrophones, equally spaced at 2.5 m, which span the central 50 m of the 100-m water column. A relatively high value (10 dB) of signal-to-noise ratio on each hydrophone was chosen in order to study source localization without concern about noise contamination.

The effect of swell and/or tidal changes on matched-field processing in shallow water are simulated by under- or overestimating the water depth in the perturbed environment and then comparing the associated acoustic fields with the unperturbed situation. In this study, the sinusoidal profile of the swell is discretized into 72 points equally spaced in phase angle at intervals of 5° along a sine wave with peak-to-trough amplitude of 7 m.

The pressure fields at the vertical hydrophone array due to estimated source positions within a range interval of 1–7 km and a depth interval of 0–100 m were obtained using the Pekeris waveguide model. Range and depth grid point separations were chosen to be 50 and 1.2 m, respectively. From this large-scale grid, the overall character of the ambiguity surface can be observed. The general height and shape of local maxima can be determined and the statistical nature of the background can be quantified. From these, estimates of output peak-to-background ratio (PBR) can be calculated. In this study, the PBR was defined as $(P - \mu)/\mu$ expressed in dB, where P is the height of the primary peak on the surface and μ is the average background level of the surface, excluding a small interval around the peak. For all cases considered, a second set of calculations was made over a finer range-depth grid centered on the expected source location. This fine grid was chosen to have resolutions of 10 m in range and 0.12 m in depth. The purpose of this effort was to provide detailed definition of the position of the ambiguity surface peak to facilitate tracking.

A synthetic set of "measured" data for each of the 37 unique swell heights was generated by running the Pekeris model to obtain the field at the receiver array due to a source at the desired location. The water depth used in this instance was equal to the 100-m modeled depth plus (or minus) the swell height. For each swell-height case, an ambiguity surface in range and depth showing the degree of correlation was produced by applying the maximum-likelihood estimator to the model field and to the synthetic data. For each of the 37 mismatch cases, an output PBR was calculated using the coarse grid, and a position in range and depth was estimated using the fine grid. In addition, a composite of these surfaces was compiled by adding the individual surfaces and then taking the mean. This composite surface was intended to represent a time-averaged result over many cycles of the surface undulations.

V. RESULTS

For reference, Fig. 3 shows an isometric projection of the maximum-likelihood ambiguity surfaces generated for

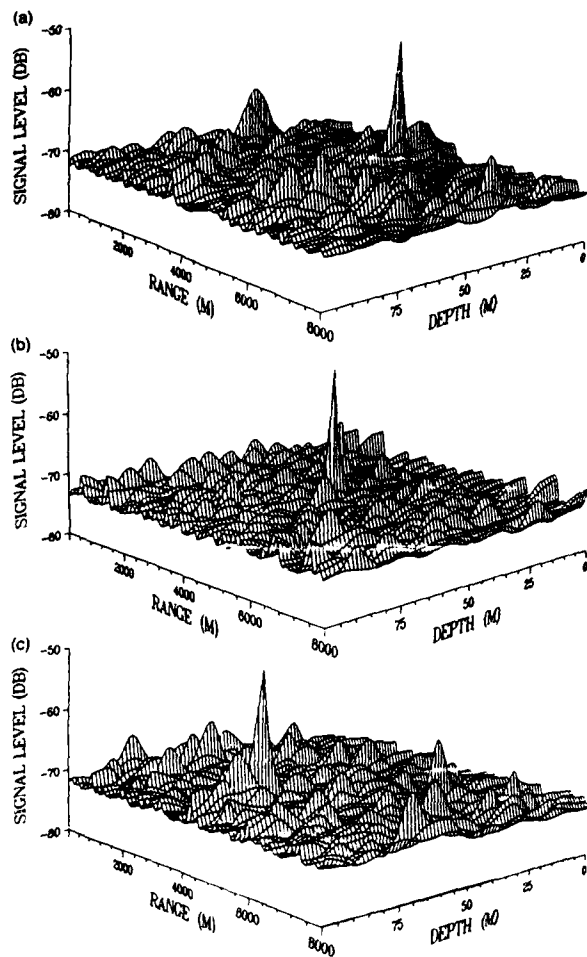


FIG. 3. Ambiguity surfaces are shown for a 150-Hz source placed at depths of: (a) 25 m, (b) 50 m, and (c) 75 m, in a 100-m Pekeris waveguide. The sea surface is assumed flat, and there is no mismatch. The input "signal"-to-noise ratio is 10 dB. The maximum-likelihood "signal" level is expressed in dB.

sources at the three chosen source depths (25, 50, and 75 m) and the fixed source range (4000 m), assuming a flat ocean surface. No mismatch between the model and "measured" sea surfaces has yet been introduced. In each case, the source peaks may be clearly seen against a background of lower secondary peaks. The value of PBR calculated on the coarse grid for these surfaces is about 20 dB for all three.

We now introduce water-depth mismatch due to swell into the problem and calculate 37 ambiguity surfaces (for each of three source depths) and then calculate the corresponding values of PBR for each. These results are presented in Fig. 4 for both 150- and 156-Hz signals. The first observation is that the best performance, in terms of output PBR, is obtained with no water-depth mismatch, as expected, and that performance degrades significantly with increasing mismatch. The second observation is that the amount of degradation is somewhat independent of source depth. The third observation is that the PBR degrades much more rapidly for negative water-depth mismatches than for positive water-depth mismatches for the 150-Hz signal. Examination of the

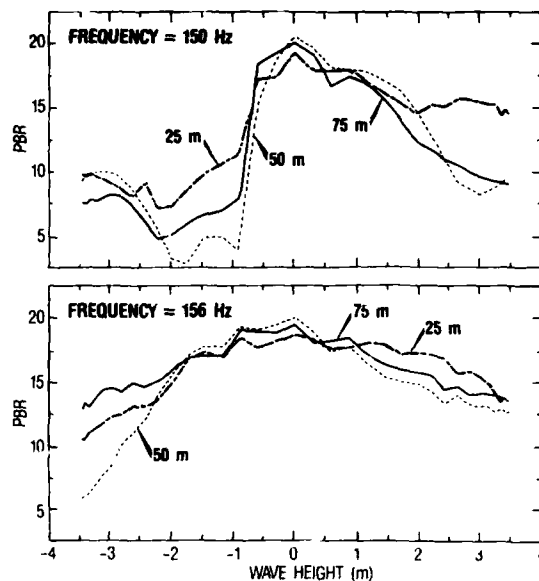


FIG. 4. Peak-to-background ratio (PBR) expressed in dB, as a function of water-depth (i.e., "wave-height") mismatch. Results are given for three source depths (25, 50, and 75 m) and two frequencies (150 and 156 Hz).

trapped normal modes at 150 Hz in this nominal 100-m waveguide shows that eight modes are supported until the water depth decreases by 0.8 m (to 99.2-m depth), at which point only seven modes are supported. When the frequency is increased to 156 Hz and the channel can then support all eight modes throughout the full range of water-depth variations, the degradation is much more gentle. The overall conclusion for Fig. 4 is that water-depth variations in shallow water will induce degradation in output PBR, and this degradation will become quite severe when there is a mismatch between the number of modes actually supported and those predicted.

Figure 5 shows the variation in range error as a function

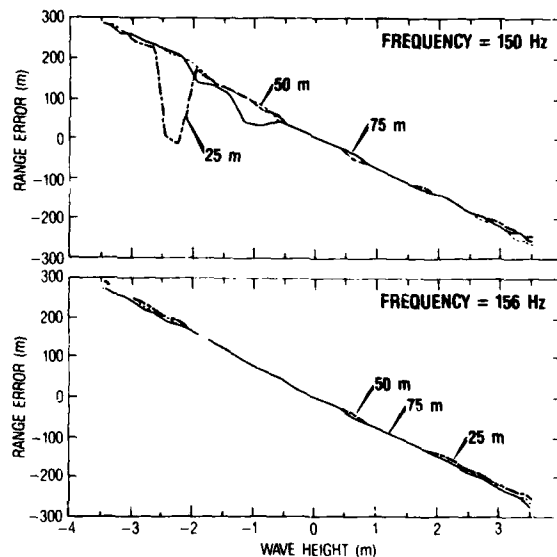


FIG. 5. Range error as a function of water-depth (wave-height) mismatch. Results are given for three source depths (25, 50, and 75 m) and two frequencies (150 and 156 Hz).

of mismatch for both 150 and 156 Hz. Inspection of this figure indicates that as the water-depth mismatch increases from negative to positive values, the range error tends to decrease linearly and monotonically for all source depths. This means that, if the water depth is overestimated in the model data, there will always be a tendency to localize the source farther away than it actually is. If the water depth is underestimated, the source will appear too close. The figure shows that, for a water-depth mismatch of ± 3.0 m ($\pm 3\%$ of the total water depth), the range error for this environment will be ∓ 250 m ($\sim \mp 6.2\%$ of the actual range). It will be noted that a few anomalous points do not fall on the main linear sequence on the negative mismatch side of Fig. 5 at 150 Hz. This is due to the loss of one of the trapped normal modes at a mismatch of -0.8 m. The value of PBR decreases by about 10 dB (see Fig. 4), and the source peak cannot, in some cases, be accurately identified from among many background peaks of similar height. We notice that, at 156 Hz, where all eight modes are supported for all values of mismatch, the range solution is very stable and undoubtedly predictable.

Figure 6 shows the variation in depth error as a function of mismatch for both 150 and 156 Hz. Apart from some obviously anomalous points at negative mismatch values (which arise for the same reason as in Fig. 5), there is a small tendency for the depth error to increase from a negative to a positive value as the water-depth mismatch increases in the same direction. Therefore, if the water depth is overestimated, there will be a tendency to localize the source shallower than it actually is, and vice versa. Inspection of the figure shows, however, that any depth errors introduced by water-depth mismatch are proportionally much smaller than the corresponding range errors. In fact, a $\pm 3\%$ error in water depth produces only a $\pm 2.5\%$ error in estimated source depth.

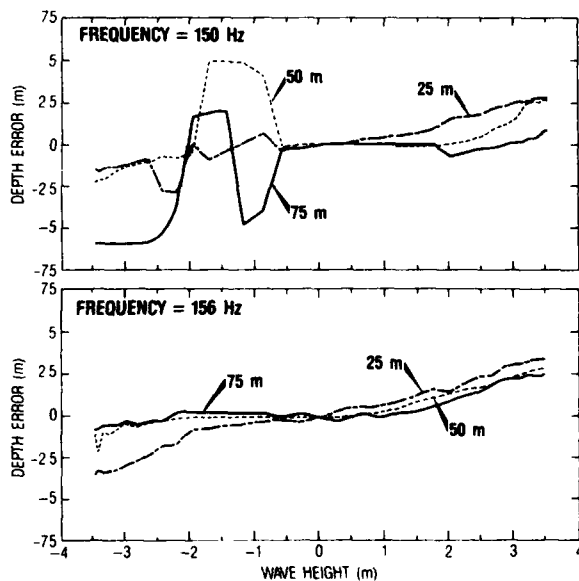


FIG. 6. Depth error as a function of water-depth (wave-height) mismatch. Results are given for three source depths (25, 50, and 75 m) and two frequencies (150 and 156 Hz).

The range and depth localization errors can be seen more dramatically when the estimated positions are viewed in the range-depth plane. Figure 7 shows the apparent location of the source for all values of mismatch considered and all three source depths at a frequency of 156 Hz. For ease of comparison, the 25- and 75-m source depth cases are normalized to the 50-m depth case. As discussed earlier, the apparent location of the source is closer and deeper than the actual location for positive water-depth mismatches. Conversely, the source appears farther away and shallower than the actual location for negative water-depth mismatches.

Figure 8 shows the composite ambiguity surfaces, calculated by taking the mean of the 72 surfaces for the individual swell heights at 5° intervals on the sine wave, as described earlier, for all three source depths. These composites represent the ambiguity surfaces obtained by averaging over one or more complete cycles of a long-period ocean swell. Inspection of these surfaces reveals that the source peaks, although degraded in quality against the corresponding peaks for the zero water-depth mismatch case in Fig. 3, are still quite identifiable. Whereas the peaks in Fig. 3 all had a value of PBR of around 20 dB, the values here are about 6.5 dB for all three source-depth cases. When comparing Fig. 8 with Fig. 3, the change of scale on the signal level axis should be noted.

The fact that the composite peaks are still clearly identifiable is rather surprising in light of the degradation due to water-depth mismatch that we have observed. The reason is as follows. For mismatches of 1–3 m, we have seen that the amplitude of the peak can fall by 10 dB or more, especially when a mode is stripped away. This means that, when the mean of the 72 surfaces is taken to obtain the composite, the surfaces for the more extreme mismatches (1–3 m) will con-

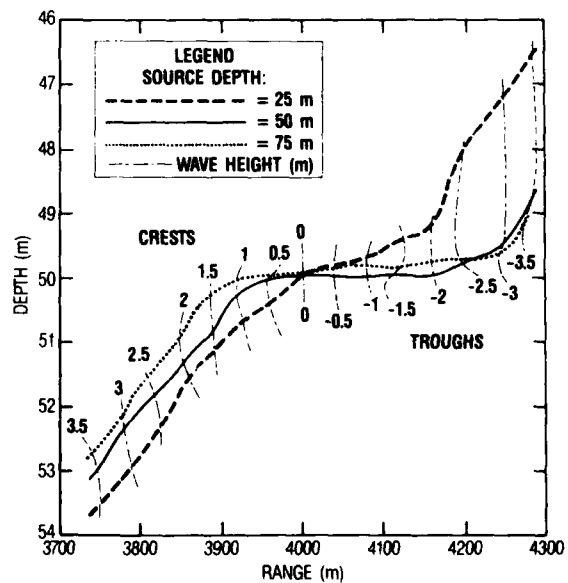


FIG. 7. Combined range and depth source localization as a function of water-depth (wave-height) mismatch. Results are for three source depths (25, 50, and 75 m) and one frequency (156 Hz). All three source depth cases are normalized to 50 m for ease of display.

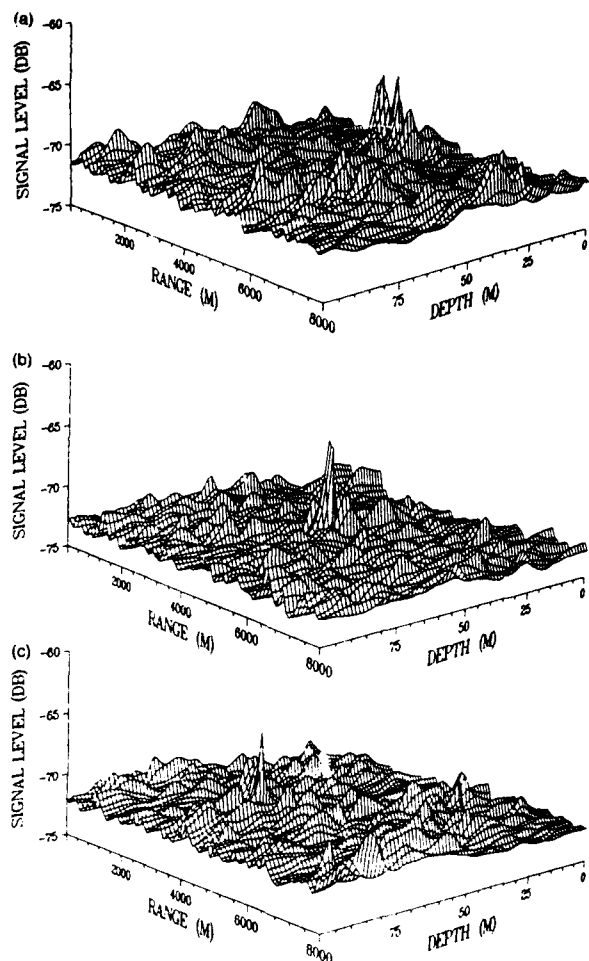


FIG. 8. Composite ambiguity surfaces for source depth cases: (a) 25 m, (b) 50 m, and (c) 75 m. The frequency is 150 Hz, and the signal-to-noise ratio is 10 dB. The maximum-likelihood "signal" level is expressed in dB.

tribute relatively little in comparison to those for near-zero (< 1 m) mismatches. Since the more extreme cases give rise to the greatest problems in peak identification and range and depth errors, the fact that they are quite naturally deemphasized is fortunate. Processing of the composite surfaces reveals zero range and depth errors for all three source depth cases, with the single exception of a range error of 0.1 km in the 50-m case.

VI. CONCLUSIONS AND RECOMMENDATIONS

We have seen that, in a shallow-water environment, significant errors can be introduced into the range and depth localization predictions of a matched-field processor through erroneous estimates of the water depth. If the water depth is overestimated, the processor will localize the source too far away and too shallow. If the depth is underestimated, the source will be seen too close and too deep. In the case examined here, percentage range errors appear to be significantly greater than percentage depth errors.

It was discovered that the output of the matched-field processor degraded more quickly with a mismatch in the number of trapped normal modes than simply with a mis-

match in the water depth. The localization solutions became unstable as soon as the water depth decreased enough to strip away one normal mode (reducing the number of modes from eight to seven).

For a composite ambiguity surface, representing an average over many cycles of a sinusoidal ocean swell, the loss in performance of the matched-field processor is dramatic (~ 14 dB) but not so bad as to preclude source identification and localization for the 10-dB input signal-to-noise ratio and the 21-element array under study. This is because the output peak-to-background ratio is dominated by the zero and near-zero mismatch ambiguity surfaces for which range and depth errors are small.

It is rather extreme to suppose that the entire sea surface between source and receiver rises and falls simultaneously. Actually, the surface will contain many perturbations between the source and receiver over a range of wavenumbers, with average mismatch close to zero. Scattering will occur from these waves, and the overall degenerative effects on the ambiguity surface may be very different from those observed under the conditions imposed by this study. The need is clearly seen for a more realistic study, allowing for random surface perturbations at various wavenumbers and orientations to the plane of acoustic propagation.

ACKNOWLEDGMENTS

This work was supported by the ASW Environmental Acoustic Support (AEAS) Program Office and by the Naval Ocean Research and Development Activity. Graphical software support was furnished by Henry Rosche III. The authors wish to acknowledge the oceanographic advice of R. L. Pickett. They also wish to thank Beverly Oxenrider, Cheri Ruffin, and Debbie Flanagan for invaluable typing assistance.

- ¹R. G. Fizell, "Application of high-resolution processing to range and depth estimation using ambiguity function methods," *J. Acoust. Soc. Am.* **82**, 606-613 (1987).
- ²R. M. Heitmeyer, W. B. Moseley, and R. G. Fizell, "Full field ambiguity processing in a complex shallow water environment," in *High-Resolution Spatial Processing in Underwater Acoustics*, edited by R. A. Wagstaff and A. B. Baggeroer (NORDA, NSTL, MS).
- ³H. P. Bucker, "Use of calculated sound fields and matched-field detection to locate sound sources in shallow water," *J. Acoust. Soc. Am.* **59**, 368-373 (1976).
- ⁴J. Capon, R. J. Greenfield, and R. J. Kolker, "Multidimensional maximum-likelihood processing of a large aperture seismic array," *Proc. IEEE* **55**, 192-211 (1967).
- ⁵M. J. Hinich, "Maximum-likelihood signal processing for a vertical array," *J. Acoust. Soc. Am.* **54**, 499-503 (1973).
- ⁶C. Feuillade and W. A. Kinney, "Source localization using a matched-field technique," *J. Acoust. Soc. Am. Suppl.* **1** **78**, S30 (1985).
- ⁷R. G. Fizell and S. C. Wales, "Source localization in range and depth in an Arctic environment," *J. Acoust. Soc. Am. Suppl.* **1** **78**, S57 (1985).
- ⁸E. R. Kanasewich, "The maximum likelihood method of spectral estimation," in *Time Sequence Analysis in Geophysics* (University of Alberta, Alberta, Canada, 1981), pp. 177-183.
- ⁹C. L. Pekeris, "Theory of propagation of explosive sound in shallow water," *Geol. Soc. Am. Mem.* **27**, 43-64 (1948).
- ¹⁰L. E. Kinsler, A. R. Frey, A. B. Coppens, and J. V. Sanders, *Fundamentals of Acoustics* (Wiley, New York, 1982), 3rd ed., pp. 434-440.
- ¹¹R. L. Wiegel, *Oceanographical Engineering* (Prentice-Hall, Englewood Cliffs, NJ, 1964), pp. 195-237.
- ¹²M. D. Earle, K. A. Bush, and G. D. Hamilton, "High-height long-period ocean waves generated by a severe storm in the Northeast Pacific Ocean during February 1983," *J. Phys. Ocean.* **14**, 1286-1299 (1984).